Available online at www.sciencedirect.com
SCIENCE DIRECT®
Journal of Power Sources 119–121 (2003) 621–625
JOURNAL OF POWER SOURCES
www.elsevier.com/locate/jpowsour

Anode properties of calcite-type MBO_3 (M:V, Fe)

Shigeto Okada*, Toshiyuki Tonuma, Yasushi Uebo, Jun-ichi Yamaki

Institute of Advanced Material Study, Kyushu University, 6-1 Kasuga Koen, Kasuga 816-8580, Japan

Abstract

V(III) was substituted in place of Fe(III) in the calcite $FeBO_3$ matrix to reduce the charge/discharge voltage and increase the theoretical capacity. The mean charge/discharge voltage of the calcite VBO_3 was 1 V lower than that of $FeBO_3$, and the reversible capacity was 420 mAh/g. To investigate the characteristics of borate anodes, the X-ray Rietveld, XPS and XAFS profiles were measured. To further improve the anode performance of VBO_3, a carbon coating using a naphthalene-based isotropic pitch with a low-temperature softening point was applied.

Keywords: Anode properties; MBO_3; Calcite; $FeBO_3$; VBO_3

1. Introduction

Polyanionic compounds such as NASICON-type $Fe_2(SO_4)_3$ and $Li_3Fe_2(PO_4)_3$ [1] have engendered much interest as rare-metal-free cathodes for next-generation lithium secondary batteries. In addition, iron borates such as Fe_3BO_6 and $FeBO_3$ [2,3] are of much interest as anode materials. The skeleton structures built up from the combination of MO_6 octahedra and XO_n polyhedral anions allow both the redox potential energy and the electrochemical properties to be tuned.

In various iron-based polyanionic cathode or anode materials, ferric borates with the lightest weight boron polyoxoanions are attractive. The theoretical capacities estimated by Fe^{3+}/Fe^{2+} redox reaction are 234 mAh/g (856 mAh/cm^3) for calcite $FeBO_3$. The volumetric capacity of $FeBO_3$ equals to that of graphite anode (855 mAh/cm^3). If the isostructural VBO_3 can be synthesized, the theoretical capacity become 893 mAh/cm^3. In addition, the 1.6 V mean voltage on lithium intercalation into ferric borates is unfortunately too high for anodic use in lithium-ion batteries. On the analogy of the 3.6 V NASICON cathode, $Fe_2(SO_4)_3$ and 2.6 V NASICON cathode, $V_2(SO_4)_3$, the mean charge/discharge voltage of VBO_3 should be 1 V lower than that of $FeBO_3$.

In this paper, we tried to design a polyanionic anode with the BO_3 group and to synthesize it with a suitable large capacity and low redox potential as an anode by chemical substitution in place of $FeBO_3$.

2. Experimental

A mixture of Fe_2O_3 and H_3BO_3 was preheated at 670 °C for 1 day and then heated for another 2 days at 750 °C in air with intermittent grinding. Better results were obtained with a large excess of H_3BO_3 than with stoichiometric H_3BO_3 but unreacted boron oxide was removed by washing with distilled water. Vanadium substituting for $FeBO_3$, with V_2O_3 as the source of vanadium, yielded similar conventional solid-state reactions. The firing was done at 670 °C for 1 day and then at 1200 °C for 1 day in Ar with 5% H_2 to avoid oxidation of the V^{3+}.

Fe_3BO_6 was obtained by a similar solid-state synthesis route, but the final synthesis temperature was 900 °C rather than 750 °C, in accordance with the report of Joubert et al. [4].

To improve the cycle performance of VBO_3, carbon coating was tried using a naphthalene-based isotropic pitch (Mitsubishi Gas Chemical Co. Inc.). The softening temperature is 86 °C. VBO_3 powders with 20 wt.% pitch were mixed and heated at 700 °C for 6 h in an electric tube furnace filled with an Ar + 5% H_2 atmosphere.

The obtained powders were indexed by XRD (Rigaku RINT2100HLR/PC), using monochromatized Cu Kα radiation. The structural parameters were refined by Rietveld analysis using RIETAN 97β [5].

The electrochemical anode performances were evaluated in coin-type cells (type 2032 made from SUS316) with a non-aqueous electrolyte (1 M $LiPF_6$/EC:DMC = 1 : 1 in volume, Tomiyama Pure Chemical Industries Ltd.) and a polypropylene separator (Celgard 3501 or 2500) against a Li metal counter electrode. These cells were disassembled in a

* Corresponding author. Tel.: +81-92-583-7841; fax: +81-92-583-7841.
E-mail address: s-okada@cm.kyushu-u.ac.jp (S. Okada).

0378-7753/03/$ – see front matter
doi:10.1016/S0378-7753(03)00308-2

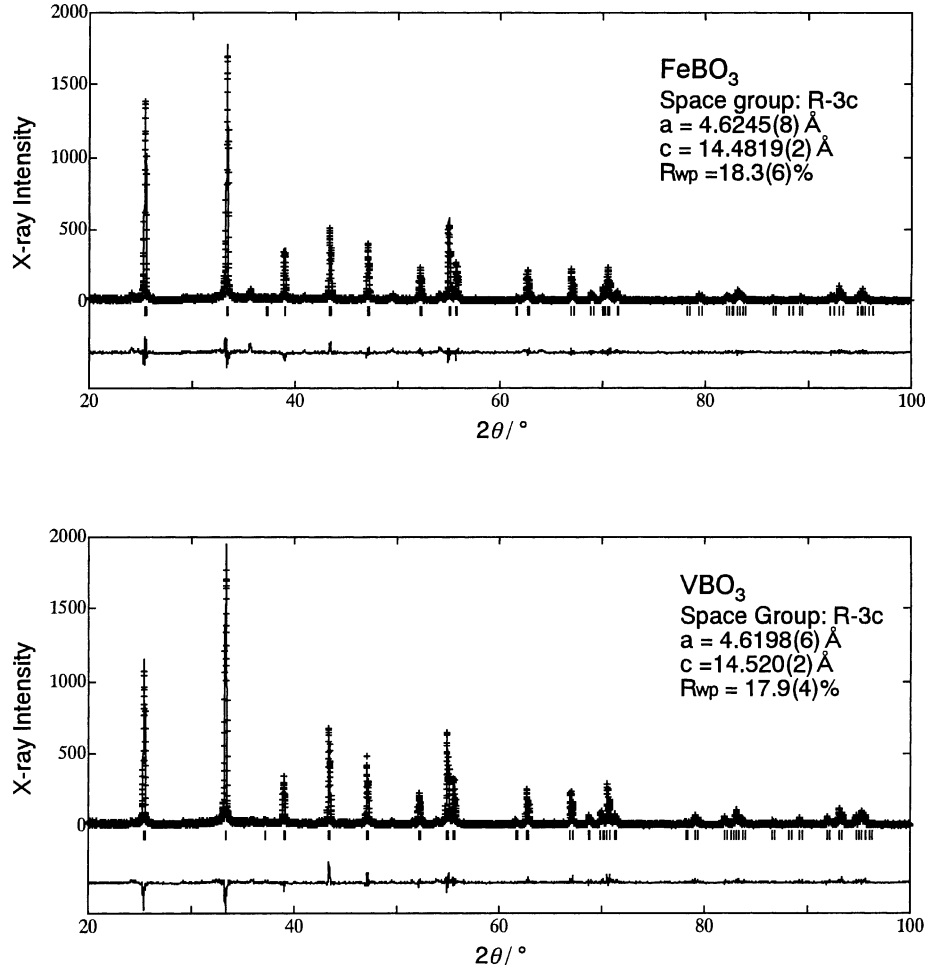

Fig. 1. Observed, calculated and difference plots for X-ray diffraction patterns of $FeBO_3$ and VBO_3.

glove box to remove the pellets that contained the active material MBO_3, acetylene black (Denki Kagaku Co. Ltd.) and F-210L PTFE Teflon binder (Daikin Industry Ltd.) in a weight ratio of 70:25:5.

X-ray photoelectron spectroscopy (XPS) for Fe in iron complex electrode materials were carried out with a JPS-9000 (JEOL Ltd.) using Mg Kα radiation. The binding energy was calibrated according to the C 1s level (284.0 eV). The pressure of the analysis chamber was less than 1×10^{-6} Pa. The analysis energy was set to 50 eV, and the tube voltage was 10 kV.

Fe K-edge X-ray absorption fine structure (XAFS) measurements were also done by transmission mode using a laboratory-type XAFS facility (Rigaku R-XAS Looper). An X-ray generator with a Mo anode and a LaB_6 cathode was operated at a voltage of 14 kV and a current of 40 mA. The incident X-ray beam was monochromatized using a Ge (2 2 0) crystal.

The Li contents in charged and discharged cathode pellets on the first cycle were measured by atomic absorption spectroscopy (Hitachi Z-5310) after the Li was dissolved using nitric acid.

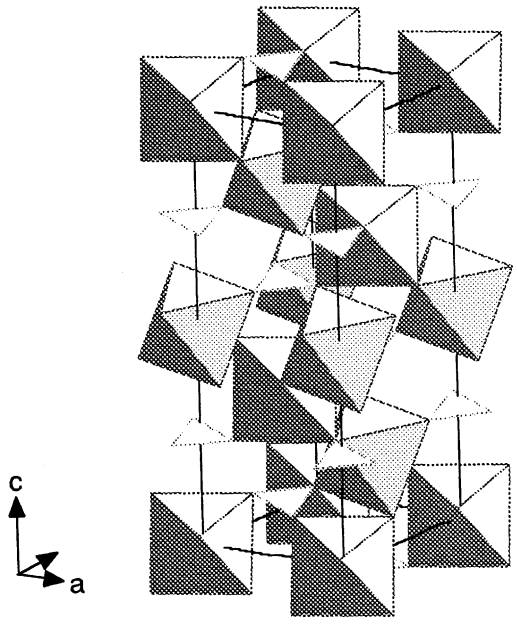

Fig. 2. Schematic diagram of $R\bar{3}c$ VBO_3 calcite structure.

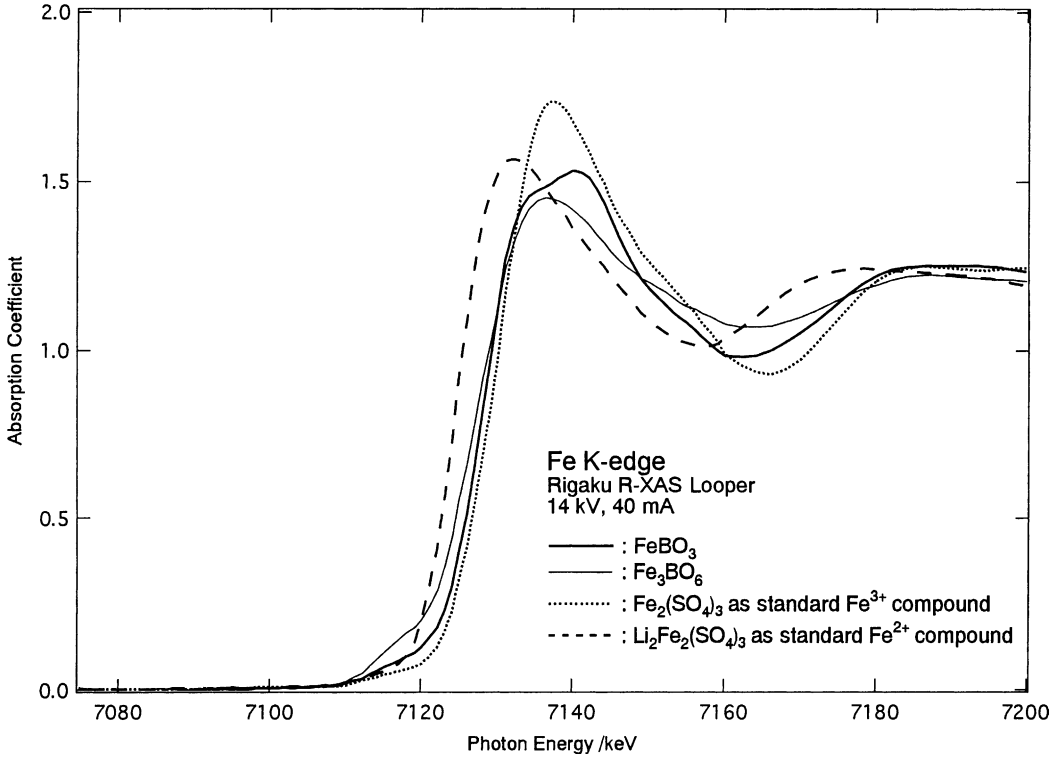

Fig. 3. Fe K-edge XANES spectra of ferric borates, sulfate and ferrous sulfate.

3. Result and discussion

We indexed the X-ray diffraction patterns of the light brown $FeBO_3$ and Fe_3BO_6 powders to, respectively, a hexagonal unit cell with $R\bar{3}c$ ($a = 4.6245(8)$ Å, $c = 14.4819(2)$ Å) and an orthorhombic unit cell with *Pnma* ($a = 10.039(15)$ Å, $b = 8.527(14)$ Å, $c = 4.4622(7)$ Å). As shown in Fig. 1, all of the peaks well matched those

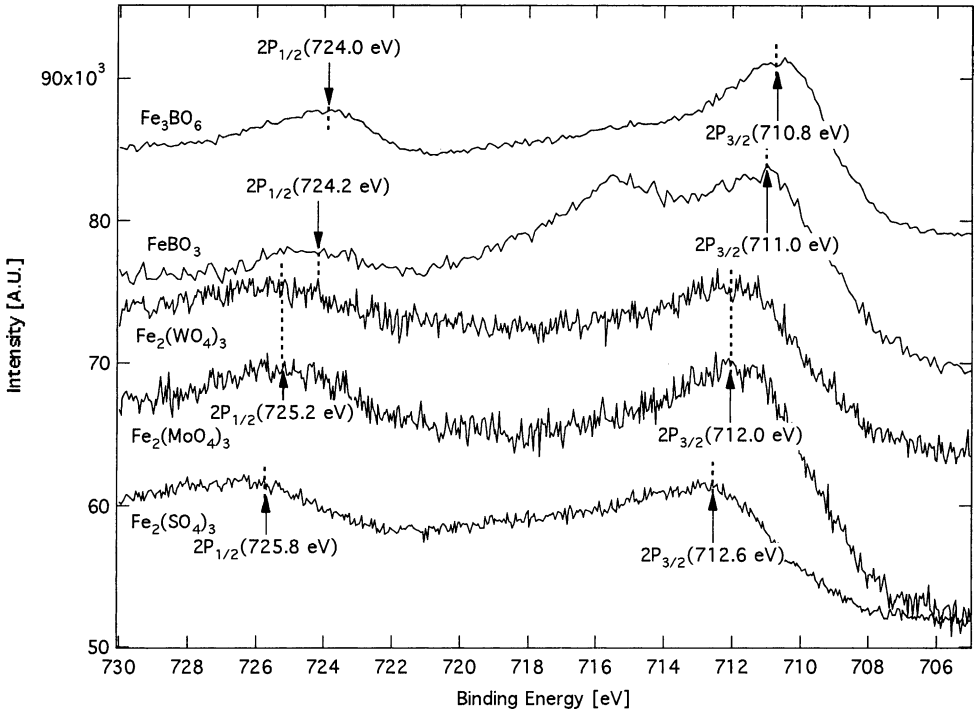

Fig. 4. XPS spectra of Fe 2p for the ferric polyanionic compounds.

Table 1
Typical 3D active materials with Fe^{3+}/Fe^{2+} redox couple

Active material	Structure	Polyoxoanion	Theoretical capacity (mAh/g)	Electronegativity of counter cation	Binding energy (eV)		Discharge voltage vs. Li/Li^+ (V)
					Fe $2p_{1/2}$	Fe $2p_{3/2}$	
Fe_2O_3 [6]	Corundum	O^{2-}	336	–	–	–	1.2
Fe_3O_4 [6]	Spinel	O^{2-}	231	–	–	–	1.2
Fe_3BO_6 [2]	Norbergite	$(BO_4)^{5-}$	293	2.04	724.0	710.8	1.6
$FeBO_3$ [2]	Calcite	$(BO_3)^{3-}$	234	2.04	724.2	711.0	1.6
$LiFePO_4$ [7]	Olivine	$(PO_4)^{3-}$	170	2.19	–	–	3.3
$Fe_2(MoO_4)_3$ [8]	NASICON	$(MoO_4)^{2-}$	91	2.35	725.2	712.0	3.0
$Fe_2(WO_4)_3$ [9]	NASICON	$(WO_4)^{2-}$	63	2.36	725.2	712.0	3.0
$Fe_2(SO_4)_3$ [8]	NASICON	$(SO_4)^{2-}$	134	2.58	725.8	712.6	3.6

given for $FeBO_3$ in the ICDD powder diffraction card no. 21-0423, with no extra peaks. The XRD profile of the obtained black VBO_3 powder agreed with that of $FeBO_3$ rather than with the ICDD powder diffraction pattern (no. 17-0311) of VBO_3. It was well refined by Rietveld analysis based on the crystal parameters of $FeBO_3$. The fitting results are illustrated in Fig. 1. The schematic diagram of the VBO_3 calcite structure obtained by Rietveld refinement is shown in Fig. 2. We expect that the corner-sharing 3D matrix of the metal borates should be suitable for anode of not only lithium-ion batteries but also sodium-ion batteries.

Fig. 3 shows the XANES spectra corresponding to the Fe K-edge for iron borates with $Fe_2(SO_4)_3$ as the standard ferric compound and lithiated $Li_2Fe_2(SO_4)_3$ as the standard ferrous compound. The shift to a higher energy peak is seen in lithiated $Li_2Fe_2(SO_4)_3$, while there is no significant difference between the peak positions of iron borates and those of $Fe_2(SO_4)_3$. This indicates that the valence states of Fe are 3+ in $FeBO_3$ and Fe_3BO_6.

XPS measurements were taken for ferric compounds such as Fe_3BO_6, $FeBO_3$, $Fe_2(MoO_4)_3$, $Fe_2(WO_4)_3$ and $Fe_2(SO_4)_3$. The Fe 2p binding energy showed a good correlation between the electronegativity of the counter cation X and the redox potential of Fe^{3+}/Fe^{2+} versus lithium as shown in Fig. 4. Hetero atoms such as B, Mo, W and S share a common oxygen nearest neighbor with Fe in an Fe–O–X linkage in a polyanionic matrix. The stronger the X–O bonding (S–O > Mo–O=W–O > B–O), weakens the Fe–O bonding via the inductive effect, hence the higher redox potential of Fe^{3+}/Fe^{2+} versus lithium. It is significant that the 1.8 eV difference between the Fe 2p binding energy of ferric sulfate and that of ferric borates reflects a 2 V difference in the cell voltage on the low rate discharge/charge profile as shown in Table 1.

The OCV for rhombohedral $Fe_2(SO_4)_3$ is about 1 V higher than that of $V_2(SO_4)_3$ [10]. Analogously, we tried to replace the redox couple from Fe^{3+}/Fe^{2+} to V^{3+}/V^{2+} in calcite $FeBO_3$. The charge/discharge profile in Fig. 5 shows that the reversible capacity of VBO_3 is 420 mAh/g and that, as we expected, the mean voltage of VBO_3 is 1 V lower than that of $FeBO_3$. Looking at the redox potentials, we see that VBO_3 should perform better than iron borate as an anode material.

The first Li insertion capacity of VBO_3 down to 0.2 V was 910 mAh/g, corresponding to $Li_{3.72}VBO_3$. The Li content from this electrochemical lithiated pellet, as detected by atomic absorption analysis, was 3.35 per VBO_3. On the next Li extraction process up to 2.5 V, 2.3 Li extraction was confirmed by atomic absorption analysis. On the other hand, the capacity of 522 mAh/g corresponds to 2.15 Li extraction. The discrepancy between the Li contents detected in the pellets and the Li contents calculated from charge/discharge capacities was <10%.

The cycleability of VBO_3 could be improved by a carbon-coating technique using a 20 wt.% naphthalene-based isotropic pitch with a low-temperature softening point. The typical cycling performance of carbon-coated VBO_3 is shown in Fig. 6.

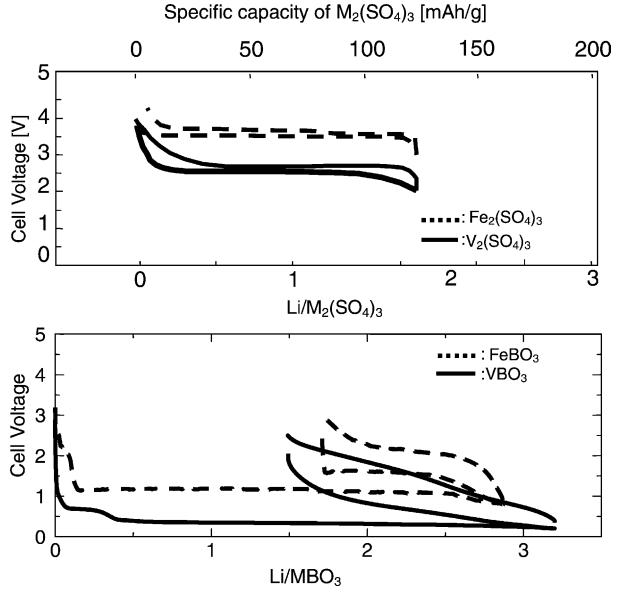

Fig. 5. Comparison of the first cycle profiles of borates and sulfates at a rate of 0.2 mA/cm^2.

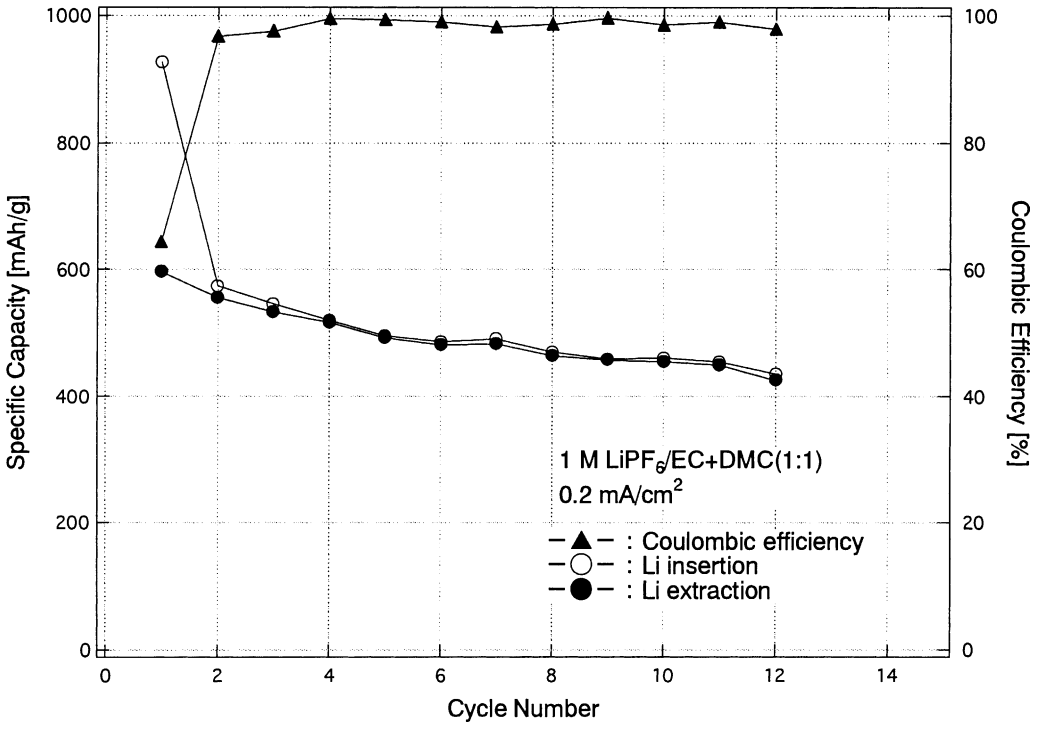

Fig. 6. Cycleability of carbon-coated VBO_3 at a rate of 0.2 mA/cm^2.

4. Conclusion

Calcite $FeBO_3$ and the isotypic VBO_3 were synthesized. The voltage difference between $FeBO_3$ and VBO_3 was 1 V. A similar discrepancy was observed in NASICON $Fe_2(SO_4)_3$ and $V_2(SO_4)_3$. From the standpoint of the charge/discharge voltage, VBO_3 should be a more suitable anode than $FeBO_3$.

Acknowledgements

The present work was partially supported by a Grant-in-Aid for the Development of Innovative Technology from the Ministry of Education, Culture, Sports, Science and Technology of Japan. The authors are grateful to Dr. Yoshinori Miura of Kyushu University for his assistance with XPS measurements.

References

[1] S. Okada, K.S. Nanjundaswamy, A. Manthiram, J.B. Goodenough, H. Ohtsuka, H. Arai, J. Yamaki, in: Proceedings of the 36th Power Sources Conference, 6–9 June 1994, pp. 110–116.
[2] J.L.C. Rowsell, J. Gaubicher, L.F. Nazar, J. Power Sources 97/98 (2001) 254–257.
[3] Ibarra-Palos, C. Darie, O. Proux, J.L. Hazemann, L. Alden, J.C. Jumas, M. Morerette, P. Strobel, Chem. Mater. 14 (2002) 1166–1173.
[4] J.C. Joubert, T. Shirk, W.B. White, R. Roy, Mater. Res. Bull. 3 (1968) 671–676.
[5] F. Izumi, in: R.A. Young (Ed.), The Rietveld Method, Oxford University Press, Oxford, 1993 (Chapter 13).
[6] M.M. Thackeray, W.I.F. David, J.B. Goodenough, Mater. Res. Bull. 17 (1982) 785–793.
[7] A.K. Padhi, K.S. Nanjundaswamy, J.B. Goodenough, J. Electrochem. Soc. 144 (1997) 1188–1194.
[8] R. Manthiram, J.B. Goodenough, J. Power Sources 26 (1989) 403–409.
[9] A. Nadiri, C. Delmas, R. Salmon, P. Hagenmuller, Rev. Chim. Miner. 21 (4) (1984) 537–544.
[10] K.S. Nanjundaswamy, A.K. Padhi, J.B. Goodenough, S. Okada, H. Ohtsuka, H. Arai, J. Yamaki, Solid State Ionics 92 (1996) 1–10.